Bases for Understanding Polymerization under Pressure: The Practical Case of CO_2

J. Contreras-García and Á. Martín Pendás

Departamento de Química Física y Analítica, Universidad de Oviedo, E-33006 Oviedo, Spain

B. Silvi

Laboratoire de Chimie Théorique, Université Pierre et Marie Curie, F-75252 Paris, France

J. M. Recio*

Departamento de Química Física y Analítica, Universidad de Oviedo, E-33006 Oviedo, Spain

Received: August 4, 2008; Revised Manuscript Received: November 1, 2008

We present a novel quantitative strategy for monitoring chemical bonding transformations in solids from the topology of their electronic structure. Developed in the context of the electron localization function formalism, it provides an unambiguous characterization of long-range interactions and bond formation. Charge flux between electron localization regions is found to hold the key for identifying the nature of the interaction between the chemically meaningful entities in the solid (valence shells, lone pairs, molecules, etc.). Because of the wide range of interesting properties that high pressure induces in molecular solids, we illustrate the potentialities of our strategy to unveil controversial questions involved in the bond reorganization along the polymerization of CO_2. Our study confirms that the topology of the bonding network in the pseudopolymeric phases points toward the incipient formation of the new bonds in the higher pressure polymers. This transformation is identified as a synchronic weakening of the intramolecular (C═O) double bond and the birth of a new intermolecular C−O bond controlled by the oxygen lone pairs. Overall, the relationship that this type of analysis establishes between different polymorphs of the phase diagram could be further exploited for the prediction of the coordination of high pressure phases, opening new avenues for experimental synthesis and structure indexation.

1. Introduction

Simple molecular solids of light elements experiment critical bonding changes toward covalent nets, and eventually to metallic structures under moderate or high pressure conditions.[1,2] Among these compounds, carbon dioxide attracts special attention not only for its relevance in many branches of fundamental and applied sciences, but also due to the controversy it has aroused in the past decade.[3,4] The rich polymorphic sequence that CO_2 develops under pressure and temperature introduces theoretical challenges in the elucidation of the microscopic factors determining the relative stability of phases. Along the progression toward polymeric structures, some intermolecular interactions must strengthen as the intramolecular C═O double bond weakens. Whether this process is synchronous or not, takes place suddenly or in a stepwise manner, in only one phase or across different phase transitions, much is not known. The lack of tools for the quantitative understanding of weak bonding interactions in real space is at the heart of these concerns.

From an applied perspective, the thermochemistry of CO_2 storage processes in environmental chemistry, as well as the search for potential superhard phases in materials engineering, would certainly benefit from an accurate evaluation and understanding of the complete phase diagram and equation of state of this compound.[5] Up to seven CO_2 phases have already been indexed, ranging from strictly molecular to polymeric three-dimensional networks.[4,6] Their range of stability, the nature of their chemical bonding, and many of their properties are the source of continuous debate. Specifically, the unexpected low compressibility of phase III, whether CO_2-II and CO_2-IV should be considered molecular phases or pseudopolymeric structures, the superhard nature of phase V, and the differences between kinetic and thermodynamic phase diagrams entail many of the discrepancies.[4,6,7] In our opinion, it is somehow shocking that rigorous analyses of their electronic structure have not yet been addressed to sustain these colorful results.

We understand that the process underlying this pressure-induced polymerization is a chemical transformation whereby cohesion in the solid changes from purely long-range electrostatic and van der Waals interactions between fragments (molecular phases) to covalency. It is our main goal to set the bases for a quantitative chemical characterization of the bonding network transformation upon polymerization. Since it is well-known that the polymerization is accompanied by an increase in electron delocalization,[1] it is reasonable to resort to the electron localization function (ELF)[8] as a quantitative tool to account for the chemical processes that take place. We will show by means of elementary quantum mechanics arguments that the attractors and bond interaction points (bips) of the ELF map play a decisive role in the analysis of the extent of the polymerization, that is, the discrimination between molecular and nonmolecular phases and the connection among polymorphs in the phase diagram. The complete characterization of the ELF topology is necessary, and information is available thanks to a new computational code developed in our laboratory. It is of general applicability in the study of bond transformations

* To whom correspondence should be addressed. Fax: (+34)985 103125; e-mail: mateo@fluor.quimica.uniovi.es.

10.1021/jp8069546 CCC: $40.75
Published on Web 01/07/2009

induced by pressure or temperature in solids.[9a,b] A short presentation of the ELF is given in the next section to illustrate the relevant features concerning the strategy to analyze these bonding changes. Results of the topological analysis in two molecular and two pseudopolymeric phases of CO_2 are discussed along the article. The paper ends with a summary of the main conclusions derived from our study.

2. Topological Approach to Long-lange Interactions

The topological approach to long-range interactions has been scarce. Probably, one of the main contributions within the atoms in molecules framework[10] has been made by Martín Pendás et al.,[11] in which bond paths are analyzed as privileged exchange channels. However, this approach becomes difficult to quantify, especially in solids, so it becomes preferable to change to the electron localization function that is defined itself as a measure of this (de)localization. The kernel of the ELF was originally defined as a local measure of the Fermi hole curvature calculated at the Hartree−Fock level,[8] and ulteriorly interpreted by Savin[12] in terms of local excess of kinetic energy due to the Pauli repulsion. The topological partition of the ELF gradient field ($\eta(\vec{r})$)[13,14] yields basins of attractors that can be thought as corresponding to atomic cores, bonds, and lone pairs. The valence basins $V(A, ...)$ encompassing a given atomic core basin $C(A)$ form the valence shell of atom A, in agreement with the Lewis's picture, and they may belong to several atomic shells. The synaptic order of a valence basin is the number of atomic shells to which it belongs. The hierarchy of the ELF basins is given by the bifurcation diagrams,[15] which provide the connectivity of the different fragments of the investigated system. The ELF value at the saddle point connecting two valence basins of separate atomic shells, the bond interaction point[16] (bips), is very useful because it tells if the connected basins belong or not to the same chemical entity. The core-valence bifurcation (CVB) index[17] is the difference of the ELF value at the saddle point between the core and the valence basins of the less electronegative atom, η_{cv}, and the ELF value at the bond interaction point, η_{vv}(bip). The CVB index is a very good criterion of the strength in hydrogen bonds[18] and can be easily generalized to the characterization of the bonding in molecular crystals.

Although the analysis of the delocalization within the ELF approach relies on the calculation of the variance and covariance of the basin populations,[19] we propose another approach based on the orbital interpretations of ELF by Burdett[20] and Nalewajski et al.[21] The value of ELF at the bip of approaching isolated fragments can be directly related to electron delocalization via the overlap (S) of the relevant orbitals involved in the interaction. As the molecules come closer, new overlaps arise between fragments, and the Pauli principle at work demands antisymmetrization of the corresponding orbitals. Following the Heitler−London approach for the orthogonalization of two interacting orbitals, let us say ϕ_i and ϕ_j, the density and the excess of kinetic energy density resulting from the interference is given, respectively, by

$$\rho = \frac{1}{1 + S^2}(\phi_i^2 + \phi_j^2 + 2S\varphi_i\varphi_j) \quad (1)$$

$$t_p = \frac{-S^2}{2(1 + S^2)}(\nabla\phi_i^2 + \nabla\phi_j^2) + \frac{S}{1 + S^2}\nabla\phi_i\nabla\phi_j. \quad (2)$$

For simplicity, we assume that the saddle point lies along the interaction line $\phi_i = \phi_j$, so the density is given by $\rho = [2(1 + S)/(1 + S^2)]\phi_i^2$, which is greater than the mere addition of both densities ($2\rho_i$). On the contrary, in the neighborhood of each of the atoms we have $\rho = [1/(1 + S^2)]\phi_i^2$ (or $\rho = [1/(1 + S^2)]\phi_j^2$), which is smaller than the corresponding initial atomic density. In other words, electrons flow from the molecule to the interfragment region as fragments approach or pressure is applied. A similar track of the kinetic energy density shows that electrons become slower in the interaction region, since the interference term is negative ($\nabla\phi_i\nabla\phi_j < 0$). As overlap (or pressure) increases, these modifications along the interaction line result in a decrease of the ratio $t_p/\rho^{5/3}$ (and hence a rise of the ELF value) at those places where it was earlier negligible, such as the first order saddle points or bips.

The spatial distribution of the critical points and their η values are therefore crucial topological quantities required to gain deeper insight into the process of bond formation involved in polymerization. Indeed, the greater the bip value, the closer the relationship between the basins involved. It would be expected that, as pressure is applied on a particular phase, charge would preferably flow only between those basins connected through bips with high ELF values.

3. Results and Discussion

The above strategy is very well adapted to investigate the evolution of the bonding in pressure-induced phase transitions. The first step required in order to investigate the changes induced in the ELF topology is the accurate characterization of the ELF critical points and basins. In this work, the ELF topological study has been performed on the all-electron crystalline wave functions of two molecular and two pseudomolecular CO_2 polymorphs computed with the CRYSTAL package.[22] Pressures associated with different volumes are evaluated from the computed energy−volume curves. All-electron calculations have been performed under the DFT framework using C and O basis sets adapted for molecular crystals[23] and Dirac−Slater exchange and Perdew−Zunger correlation functionals.[24] This choice was dictated by the proper description and convergence of delocalization interactions in the pseudomolecular phases.[25] Although it is known to affect to a little extent the results provided by the topological analysis of ELF,[26] the stability of the results has been confirmed for other computational parameters at particular geometries.

3.1. Molecular Phases. Several molecular phases have been found to exist in the phase diagram of CO_2. At ambient pressure, CO_2 solidifies in the $Pa\bar{3}$ phase I,[27] a cubic phase that transforms into the orthorhombic *Cmca* phase III at 12 GPa with almost no density change.[28] According to our topological analysis, both phases reveal a clear molecular solid, composed of CO_2 entities that maintain the C−O bond length of the molecule (1.168 Å), with small, almost spherical C and O core basins, large basins hosting the lone pair electrons, V(O) (filling up around 72% of the unit cell volume) and an arrangement of ring-shaped maxima for the C−O bonds, V(C,O) (see Figure 1). The inspection of the intramolecular bond in Figure 1 reveals a clear parallelism between the multiple bonds in the solid and the free molecule, since both of them display a ring shape.[29] However, the rupture of the $D_{\infty h}$ symmetry results in a collapse of the degenerated ring around the internuclear line into several nondegenerated maxima in the crystal.

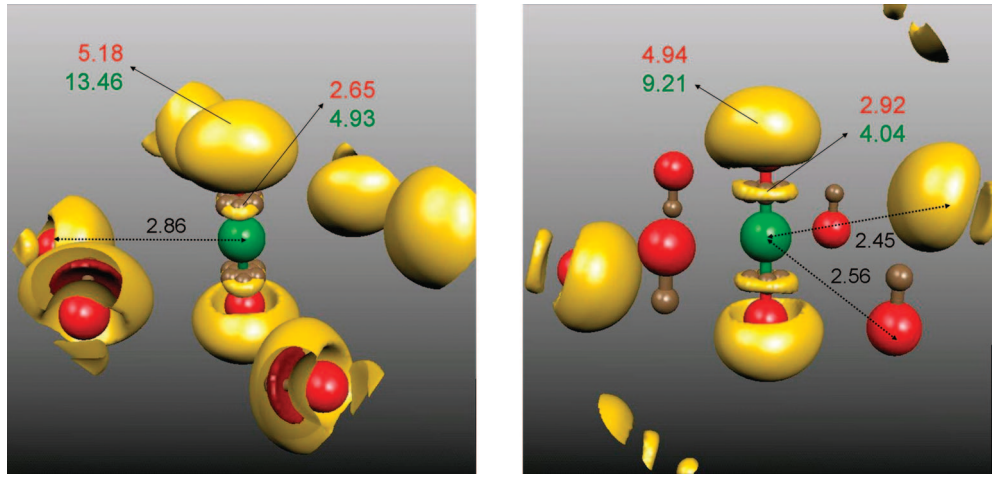

Figure 1. $\eta = 0.82$ localization domains of CO_2-I (left) and CO_2-III (right). For the sake of clarity, only one carbon and the eight nearest oxygens are represented. The central molecule displays the carbon core in green, oxygen cores in red, and valence attractors in brown. The yellow surfaces represent the oxygen lone pairs (surrounding oxygen cores) and the annular bonds (along the C−O directions). Numbers in red (green) stand for populations (in electrons) (volumes, Å^3) of the V(O) monosynaptic and V(C,O) disynaptic basins. C−O distances (in black, Å) correspond to CO_2-I and CO_2-III unit cells at 0 and 12 GPa, respectively.

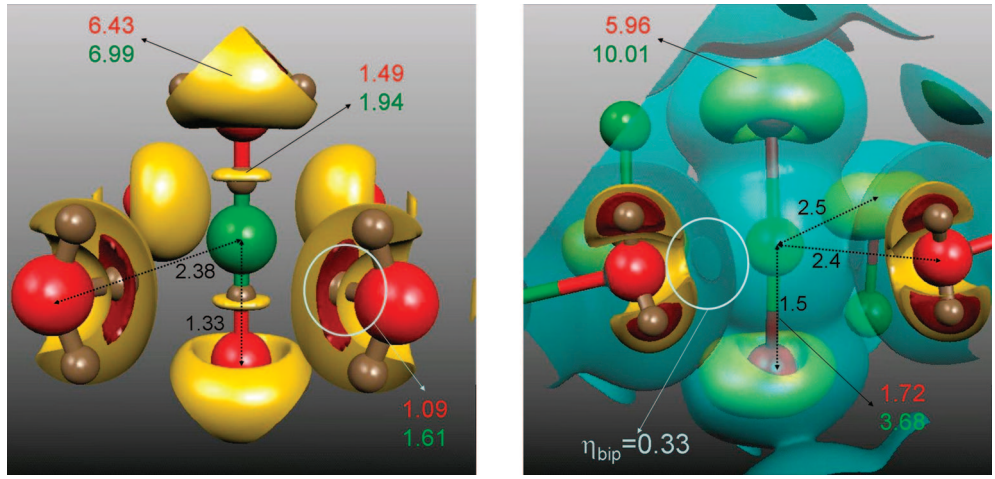

Figure 2. $\eta = 0.8$ localization domains of CO_2-II (left) and CO_2-IV (right). For the sake of clarity, only one carbon and its six nearest oxygens are represented. Colors and symbols as in previous caption. C−O distances (in black, Å) correspond to those in the CO_2-II and CO_2-IV unit cells quoted in the text. White circles and the green isosurface ($\eta = 0.3$), so as to show intermolecular relationships, highlight polymerization features explained in the text.

The molecular character of these two phases is consistent with positive CVB indexes due to the very low ELF value at the corresponding intermolecular saddle points ($\eta \simeq 0.02$ and 0.04, respectively),[30] whereas their high compressibility is explained by the great ELF flat regions between the molecular fragments, able to assume pressure without much energetic cost. The intermolecular forces that retain the CO_2 fragments together in the solid are long-range, and virtually no orbital overlap between them occurs: the main source of stabilization is the quadrupole-quadrupole attraction between CO_2 units in both cases.The lack of short-range interactions is easily inferred from the analysis of the change in the basin populations induced by compression in both phases. As pressure is applied, charge does not flow from the lone pair basins to the intermolecular region, but to the bond basins. The C−O bonds in these phases are able to accommodate incoming charge at ease since they retain the double bond character found in free CO_2 molecules. Figure 1 (right) illustrates the ELF topology at high pressure for CO_2-III in order to highlight its topological equivalence with phase I. Similar charge trends as those displayed in Figure 1 (left) were found for CO_2-I at elevated pressures. All these arguments support the molecular character of phases I and III, and stand against the suggested low compressibility of CO_2-III.

3.2. Pseudomolecular Phases. According to the experimental work reported in refs 4 and 31−33, upon subsequent heating and pressurizing of the molecular phases, CO_2 undergoes phase transitions toward the so-called pseudopolymeric structures (CO_2-II and CO_2-IV), which are suggested as precursors of extended covalent lattices, although some other experimental[3,6] and theoretical[7] investigations conclude that these phases are still molecular at their proposed stable geometries. The structure given for phase II by Yoo et al. at 28 GPa and 680 K is characterized by CO_2 subunits with an elongated intramolecular C−O distance of 1.331 Å and a second coordination sphere for carbon constituted by 4 equatorial oxygens at distances as low as 2.377 Å.[32] For CO_2-IV, we have selected the orthorhombic structure reported by Park et al.[33] that displays slightly bent CO_2 molecules (O−C−O angle of 171°), C−O distances around 1.5 Å, and short distances from C to other 2 and 4 O at 2.1 and 2.4 Å, respectively.

The ELF analysis of these phases suggests solutions to several unanswered questions, such as the chemical driving

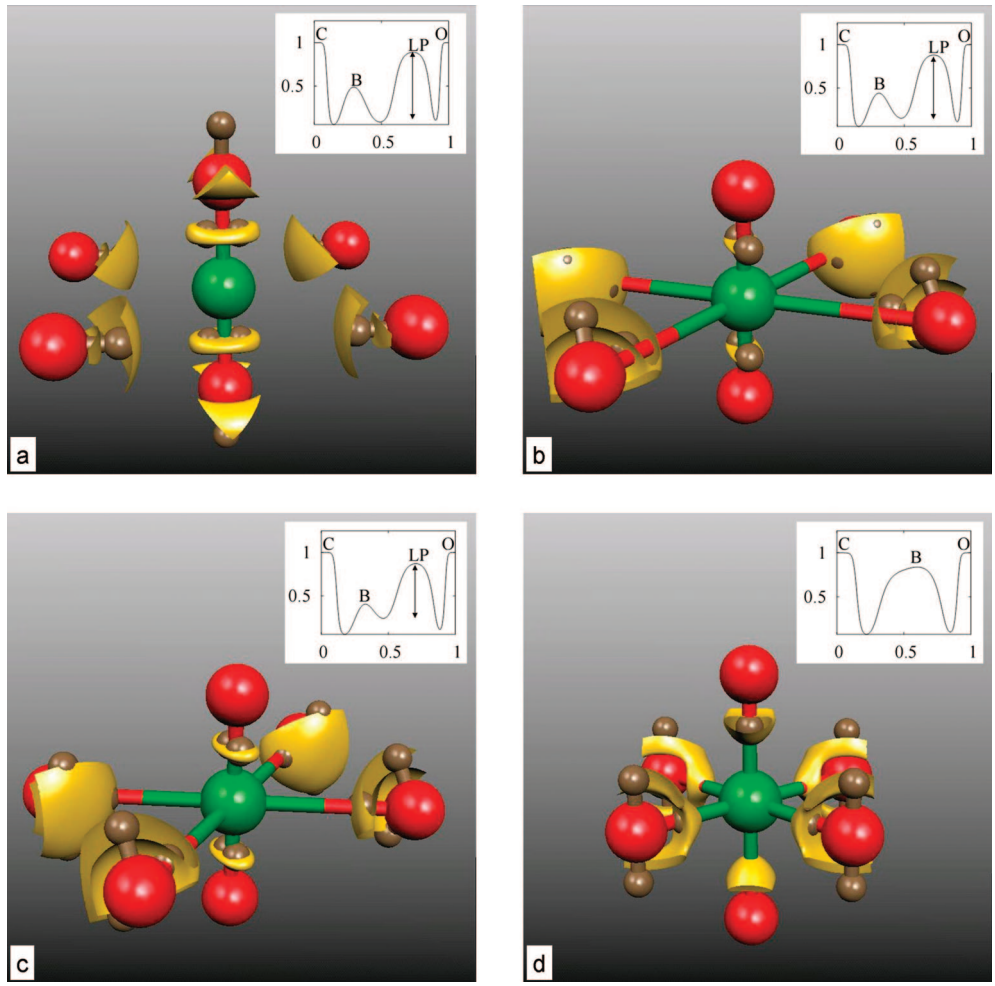

Figure 3. Changes of the ELF topology of phase II as pressure increases from a to d. Colors and symbols as in previous captions. Insets display ELF profiles along the new bonding direction using a normalized distance between the interacting fragments. Arrow lengths illustrate how $\Delta\eta^{val}$ decreases with pressure. Labels C, O, B, and LP stand for C-core C(C), O-core C(O), bond V(C,O), and lone pair basins V(O), respectively.

force underlying the polymerization, the quantification of the experimentally observed delocalization, and the progressive nature of the process. First, we focus on the results at the particular geometries given above. In the case of CO_2-II, two new basins oriented (each) toward one next nearest carbon atom emerge in the oxygen lone pair region (see the white circle in Figure 2, left). Each of these newly arisen basins can be considered as a prelude to a future bond to C, giving rise to a 3-fold coordination for O and a 2 + 4 coordination for C. This fact confirms the suggestion by Iota et al.[4] who proposed that phase II may be a precursor of the 6-fold coordinated phase VI, instead of the 4-fold coordinated phase V, as it was earlier believed. Similarly, in CO_2-IV the connection between CO_2 fragments is achieved through a saddle point whose ELF value is as large as 0.33 (see the green isosurface and the white circle in Figure 2, right). We have now a negative CVB index (−0.23), and the CO_2 fragments become chemically interacting, revealing an increasing short-range interaction between the oxygen lone pair basin and the second next-nearest carbon atom. This new interaction undoubtedly points toward CO_2-IV as a precursor of 4-fold CO_2-V.

The emerging bonding in both phases can be identified with a "secondary interaction" in classical chemistry, identified by Grochala et al.[34] as the main driver of increasing coordination under pressure. This structural feature is characterized by the interaction between a lone pair on one atom facing an orbital of the same symmetry in another molecule at a separation lower than the van der Waals radius.[35] As was pointed out in the Heitler−London bonding analysis, the antisymmetrization of these orbitals gives rise both to an electron flow and to a contraction of the orbitals upon compression. Both responses add up to give an increase of ELF in those places where it was previously negligible (the bips between fragments), coupled to a corresponding lowering in the fragment region that has been depopulated (the molecular bond) as the overlap increases. Furthermore, the different nature of the local increase in ELF within phases II and IV results in a new maximum in the former, whereas the intermolecular saddle point remains as such in CO_2-IV. This can be directly related to the different nature of the bonding they are anticipating: the greater ionicity of the 6-fold coordination structure favors the formation of a polarized interaction within phase II prior to polymerization. In contrast with the molecular phases, to explain the bonding within the CO_2 fragments of these phases we need the $CO^{2+}\cdots O^{2-}$ mesomeric structure because the V(C,O) population is now less than 2 (see Figure 2 and ref 30). Note also that the purely electrostatic energy increases because the quadrupole moments of the CO_2 fragments in the crystal increase.

Moreover, the analysis carried out so far rationalizes the experimentally observed increase in delocalization. It is enough to recall that upon compression both the valence maxima ($\eta^{val}_{(3,-3)}$) and minima ($\eta^{val}_{(3,-1)}$) along the new bonding direction tend toward the ELF value that represents the homogeneous electron gas ($\eta = 0.5$). This effect may be accounted for through the index introduced by Silvi and Gatti in their study of delocalization in metals:[36]

$$\Delta\eta^{val} = \eta^{val}_{(3,-3)} - \eta^{val}_{(3,-1)} \quad (3)$$

For phases I and III, the computed values of $\Delta\eta^{val}$ are 0.873 and 0.848, whereas for phases II and IV $\Delta\eta^{val}$ decreases to 0.794 and 0.506, respectively.

Finally, it is interesting to note that the process toward the extended phases has been claimed to be a smooth common chemical transformation that starts with a molecular-like phase and is only driven by a shortening of the distances between the approaching molecules, instead of a genuine abrupt structural phase transition.[3] Within this chemical transformation viewpoint, the progressive-wise polymerization must involve intermediate stages of pseudomolecular-like nature, as those here considered for phases II and IV. This issue merits further analysis, as follows.

The progressive formation of the covalent bond upon compression of the pseudopolymeric phase II under the static approximation is illustrated in Figure 3. The weakening of the intramolecular C−O bond is first observed in the loss of its annular shape (Figure 3a), characteristic of the strictly molecular phases, as well as in the decrease of its electron population. As the polymerization takes place, charge flows from the intramolecular bond toward the intermolecular region where the new bond is being formed. At variance with the effect of pressure in the molecular phases, the emergence of new maxima directed toward the approaching carbon (Figure 3b) constitutes the natural proof of this effect. Indeed, these new attractors progressively approach the intermolecular direction (Figure 3c), so that the path to 6-fold coordination is completed when the molecular C−O bond maxima finally collapse onto the internuclear line (Figure 3d), fingerprint of a single bond. Simultaneously and as pressure is increased, the V(O) monosynatic basin, which accounts for all the oxygen lone pairs at low pressure, is split into distinct chemically effective monosynaptic basins, some of them become ultimately disynaptic forming new CO bonds. The transformation is easily visualized in the insets of Figure 3, where the lone pair and the intramolecular bond basins are seen to evolve toward a new intermolecular bond.

4. Conclusions

Overall, we believe that the polemic analysis of the nature of pseudopolymeric phases has been centered on the geometry of the compounds, whereas little efforts have been paid to unveil their underlying electronic structures. The broadening of the ELF scope we have introduced has allowed us to prove that the specific structure of the CO_2 fragments within the crystal is not crucial in the process leading to a new polymeric structure. The electron localization function is able to characterize the pseudopolymeric nature of the bonding intermediates as well as to identify the degree of bond formation. It is able to provide interesting figures for the bases of bond formation: (i) the increase in exchange interactions, with high ELF values (as high as $\eta = 0.33$!) and (ii) the appearance of oriented maxima (secondary interactions). Moreover, it is able to describe the general bonding route leading to the polymeric phase: the rupture of intramolecular bonds and the creation of new intermolecular bonds is carried out in a synchronous manner, when the ELF value at the bips connecting CO_2 fragments is high enough to allow charge flow from the double C−O bond into the intermolecular region. In this process the qualitative transformation of the lone pair basins into bonding pairs is of capital interest to predict the coordination of the high-pressure polymorphs.

Acknowledgment. In memoriam of Professor Lorenzo Pueyo. Financial support from the Spanish MEC and FEDER programs under projects MAT2006-13548-C02-02 and CTQ2006-02976 and from the Spanish MALTA-Consolider Ingenio-2010 program under project CSD2007-00045 are gratefully acknowledged. J.C.G. thanks M. Reynés for fruitful discussions.

References and Notes

(1) Hemley, R. J. *Annu. Rev. Phys. Chem.* **2000**, *51*, 763.
(2) Erements, M. L.; Russell, R. J.; Mao, H. K.; Greforyanz, E. *Nature* **2001**, *411*, 170.
(3) Santoro, M.; Gorelli, F. A. *Chem. Soc. Rev.* **2006**, *35*, 918.
(4) Iota, V.; Yoo, C.-S.; Klepeis, J.-H.; Jenei, Z.; Evans, W.; Cynn, H. *Nat. Mater.* **2007**, *6* (34), 10022.
(5) (a) House, K. Z.; Schrag, D. P.; Harvey, C. F.; Lackner, K. S. *PNAS* **2006**, *103*, 12299. (b) Yoo, C.-S.; Cynn, H.; Gygi, F.; Galli, G.; Nicol, M.; Häusermann, D.; Carlson, S.; Mailhiot, C. *Phys. Rev. Lett.* **1999**, *83*, 5527.
(6) Giordano, V. M.; Datchi, F. *Eur. Phys. Lett.* **2007**, *77*, 46002.
(7) Bonev, S. A.; Gygi, F.; Ogitsu, T.; Galli, G. *Phys. Rev. Lett.* **2003**, *91*, 065501.
(8) Becke, A. D.; Edgecombe, K. E. *J. Chem. Phys.* **1990**, *92*, 5397.
(9) (a) Contreras-García, J.; Martín Pendás, A.; Silvi, B.; Recio, J. M. *J. Phys. Chem. Solids* **2008**, *69*, 2204. (b) Contreras-García, J.; Martín Pendás, A.; Recio, J. M.; Silvi, B. *J. Chem. Theory Comput.* **2009**, in press.
(10) Bader, R. F. W. *Atoms in Molecules. A Quantum Theory*; Clarendon Press: Oxford, UK, 1990.
(11) Martín Pendás, A. M.; Francisco, E.; Blanco, M. A.; Gatti, C. *Chem.—Eur. J.* **2007**, *13*, 9362.
(12) (a) Savin, A.; Becke, A. D.; Flad, J.; Nesper, R.; Preuss, H.; von Schnering, H. G. *Angew. Chem., Int. Ed. Engl.* **1991**, *30*, 409. (b) Savin, A.; Jepsen, O.; Flad, J.; Andersen, O. K.; Preuss, H.; von Schnering, H. G. *Angew. Chem., Int. Ed. Engl.* **1992**, *31*, 187. (c) Savin, A.; Nesper, R.; Wengert, S.; Fässler, T. F. *Angew. Chem., Int. Ed. Engl.* **1997**, *36*, 1809.
(13) Silvi, B.; Savin, A. *Nature* **1994**, *371*, 683.
(14) Häussermann, U.; Wengert, S.; Nesper, R. *Angew. Chem., Int. Ed. Engl.* **1994**, *33*, 2069.
(15) (a) Savin, A.; Silvi, B.; Colonna, F. *Can. J. Chem.* **1996**, *74*, 1088. (b) Calatayud, M.; Andrés, J.; Beltrán, A.; Silvi, B. *Theor. Chem. Acc.* **2001**, *105*, 299.
(16) Kohout, M.; Wagner, F. R.; Grin, Y. *Theor. Chem. Acc.* **2002**, *108*, 150.
(17) Fuster, F.; Silvi, B. *Theor. Chem. Acc.* **2000**, *104*, 13.
(18) Gutierrez-Oliva, S.; Joubert, L.; Adamo, C.; Bulat, F.; Zagal, J.; Toro-Labbe, A. *J. Phys. Chem. A* **2006**, *110*, 5102.
(19) Silvi, B. *Phys. Chem. Chem. Phys.* **2004**, *6*, 256.
(20) Burdett, J. K.; McCormick, T. A. *J. Phys. Chem. A* **1998**, *102*, 6366.
(21) Nalewajski, R. F.; Köster, A. M.; Escalante, S. *J. Phys. Chem. A* **2005**, *109*, 10038.
(22) Saunders, V. R.; Dovesi, R.; Roetti, C.; Causá, M.; Harrison, N. M.; Orlando, R.; Zicovich-Wilson, C. M. *CRYSTAL98 User's Manual*; University of Torino: Torino (Italy), 1998.
(23) Gatti, C.; Saunders, V.; Roetti, C. *J. Chem. Phys.* **1994**, *101*, 10686.
(24) Perdew, J. P.; Zunger, A. *Phys. Rev.* **1981**, *23*, 5048.
(25) Mori-Sánchez, P.; Cohen, A. J.; Yang, W. *Phys. Rev. Lett.* **2008**, *100*, 146401.
(26) Noury, S.; Colonna, F.; Savin, A.; Silvi, B J. *Molec. Struct.* **1998**, *450*, 59.
(27) Downs, R. T.; Somayazulu, M. S. *Acta Crystallogr. C* **1998**, *54*, 897.
(28) Aoki, K.; Yamawaki, H.; Sakashita, M.; Gotch, T.; Takemura, K. *Science* **1994**, *263*, 356.
(29) Isolated molecules with multiple bonds are characterized by a degenerated maximum of ELF surrounding the internuclear line. Silvi, B.; Savin, A. *Nature* **1994**, *371*, 683)

(30) For the sake of comparison, B3LYP/6311+(2df) calculations in the CO molecule yield $\eta_{cv} = 0.1$, $V(O) = 4.7$, and $V(C,O) = 3.09$. The variance of $V(C,O)$ is 1.52, and the $V(O)-V(C,O)$ covariance is −0.96. This is consistent with a mesomeric superperposition involving the O=C−O and O−C=O partially ionic structures in addition to O=C=O.

(31) (a) Iota, V.; Yoo, C.-S. *Phys. Rev. Lett.* **2001**, *86*, 5922. (b) Yoo, C.-S.; Iota, V.; Cynn, H. *Phys. Rev. Lett.* **2001**, *86*, 444.

(32) Yoo, C.-S.; Kohlmann, H.; Cynn, H.; Nicol, M. F.; Iota, V.; Le Bihan, T. *Phys. Rev. B* **2002**, *65*, 104103.

(33) Park, J.-H.; Yoo, C.-S.; Iota, V.; Cynn, H.; Nicol, M. F.; Le Bihan, T. *Phys. Rev. B* **2003**, *68*, 014107.

(34) Grochala, W.; Hoffmann, R.; Fenf, J.; Ashcroft, N. W. *Angew. Chem., Int. Ed.* **2000**, *46*, 3620.

(35) Landrum, G. A.; Goldberg, N.; Hoffmann, R. J. *Chem. Soc. Dalton Trans.* **1997**, 3605.

(36) Silvi, B.; Gatti, C. *J. Phys. Chem.* **2000**, *104*, 247.

JP8069546